Materials Plus
https://ojs.wiserpub.com/index.php/mp/

Research Article

Dynamic Analysis of Shaft with Variable Mechanical Property under Dynamic Load by FEM Method

Van-Luat Nguyen

Faculty of Mechanical Engineering, Hanoi University of Industry, 298 Cau Dien Street, Bac Tu Liem District, Hanoi, Vietnam
E-mail: nguyenvanluat@haui.edu.vn; luatnv1980@gmail.com

Received: 18 April 2023; **Revised:** 24 May 2023; **Accepted:** 25 May 2023

Abstract: The paper introduces the dynamic responses of a circular shaft with variable mechanical properties under dynamic loads. The direct construction of finite element formulation for dynamic problems, which include stiffness matrix, and mass matrix for circular axis. The Functionally Graded Material (FGM) shaft with material properties is assumed to vary continuously in the longitudinal direction investigated. Building a numerical program for the problem based on Bernoulli beam theory, and Newmark numerical algorithm. The obtained numerical results have found the kinematic response of the shaft with the longitudinal variation of mechanical properties under the action of dynamic loads. The results were also compared with the analytical results in some special cases to clarify the reliability of the calculation method.

***Keywords*:** spinning shaft, FGM shaft, dynamic load, FEM, frequency response

1. Introduction

The shaft is a common type of construction in most machine equipment. The oscillation of the shaft and beam with constant mechanical properties under the effect of dynamic loads has been proposed in many previous studies [1–7]. Functionally graded material (FGM) is created by continuously varying the volume fractions of the component materials, often in spatial coordinates. Thus, FGM does not have the disadvantages commonly encountered in layered and fiber-reinforced composites such as delamination or stress concentration. Combining the advantages of component materials, FGM materials are increasingly studied and widely applied in practice. Many researchers have investigated different aspects of the dynamic behavior of a rotating shaft by assuming it as a rotating Euler Bernoulli's theory. The traditional analytical methods, especially the Galerkin method are employed by researchers in studying the mechanical behavior of FGM shafts, Finite element method (FEM) is also widely used to study the behavior of FGM shafts and beams. Several finite-element beam models for the analysis of FGM beams have been proposed [8,9,10]. However, in addition to torsional strain, the shaft is also subjected to flexural deformation at the same time, which is rarely mentioned in previous studies. This study focuses on the kinematic analysis of shafts whose longitudinal mechanical properties vary by finite element method. Which includes building a finite element formulation based on a 2-node axis element with mechanical properties varying along the axis.

DOI: https://doi.org/10.37256/mp02010003

2. Elastic energy function and kinetic energy of a shaft with variable mechanical properties

Consider the circular shaft with the coordinate system being the x-axis in the direction of the circular axis and the y- and z-axes on the cross-section. The effective properties such as Young's modulus (E), shear modulus (G), and mass density (ρ) of the ceramic (c) and metal (m), respectively. The effective properties of the axially FGM beams evaluated by Voigt mode are as follows

$$E(x) = E_m v_m + E_c v_c,\ G(x) = G_m v_m + G_c v_c,\ \rho(x) = \rho_m v_m + \rho_c v_c \tag{1}$$

where E_c, E_m are the volume elastic modulus of ceramic and metal, respectively,

G_c, G_m the shear modulus of elasticity of ceramic and metal,

ρ_c, ρ_m are the mass density of ceramic and metal

v_c, v_m are the volume fraction of ceramic and metal

$$v_m = (1 - \frac{x}{L})^n,\ v_c + v_m = 1 \tag{2}$$

where n is the nonnegative grading index, and L is the length of the shaft. Based on the Euler-Bernoulli beam theory, the displacements $\bar{u}$ and ω of an arbitrary point in the x and z directions, respectively are given by

$$\begin{cases} \bar{u}(x,z,t) = u(x,t) - z\varphi(x,t) \\ \omega(x,z,t) = \omega(x,t) \\ \varphi = \dfrac{\partial \omega}{\partial x} = \omega_{,x}, \quad \theta = \theta(x,t) \end{cases} \tag{3}$$

where $u(x, t)$ and $\omega(x,t)$ are respectively the axial and transverse displacements of a point on the x-axis at the midplane, $\varphi(x,t)$ is the cross-sectional rotation, and t is the time variable, z is the distance of the midplane, θ is the angle of twist of the cross-sectional, the strain ε, γ and the stress σ can be obtained as follows [15]:

$$\varepsilon_x = \frac{\partial \bar{u}}{\partial x} = \frac{\partial u}{\partial x} - z\frac{\partial \varphi}{\partial x} = u_{,x} - z\omega_{,xx} \tag{4}$$

$$\gamma = r.\frac{d\theta}{dx} = r.\theta_{,x} \tag{5}$$

Hooke's law:

$$\sigma_x = E(x).\varepsilon_x \quad \tau_\rho = G(x).\gamma \tag{6}$$

r is the distance from any point of stress to the x-axis of the shaft

The strain energy of torsion and bending shafts for an element with an initial length of l with variable mechanical properties having a form:

$$\begin{aligned} U &= \frac{1}{2}\int_{V_e} \sigma_x \varepsilon_x dV + \frac{1}{2}\int_{V_e} \tau_\rho \gamma dV_e = \frac{1}{2}\int_0^l \int_F \sigma_x \varepsilon_x dF.dx + \frac{1}{2}\int_0^l \int_F G(x)\gamma^2 dF dx \\ &= \frac{1}{2}\int_0^l \int_F E(x)\varepsilon_x^2 dF.dx + \frac{1}{2}\int_0^l \int_F G(x) r^2 \theta_{,x}^2 dF.dx \\ &= \frac{1}{2}\int_0^l \int_F \left[E(x)u_{,x}^2 - 2.E(x)zu_{,x}\omega_{,xx} + E(x)z^2\omega_{,xx}^2 \right] dF dx + \frac{1}{2}\int_0^l \int_F G(x) r^2 \theta_{,x}^2 dF.dx \\ &= \frac{1}{2}F\int_0^l E(x)u_{,x}^2 dx + \frac{1}{2}I_y\int_0^l E(x)\omega_{,xx}^2 dx + \frac{1}{2}I_x\int_0^l G(x)\theta_{,x}^2 dx \end{aligned} \tag{7}$$

In which $\int_F z dF = 0$; $I_y = \int_F z^2 dF$, $I_x = \int_F r^2 dF$

where V_e is the volume of an element of the shaft, and A is the area of the cross-section of the shaft.

The kinetic energy of an element with an initial length of l having a form

$$T = \frac{1}{2}\int_{V_e} \rho(x)\left(\dot{\bar{u}}^2 + \dot{\omega}^2\right) dV + \frac{1}{2}\int_{V_e} \rho(x) r^2 \dot{\theta}^2 dV$$

$$= \frac{1}{2}\int_0^l \int_{F(x)} \left[\rho(x)\left(\dot{u}^2 + \dot{\omega}^2\right) + \rho(x) z^2 \dot{\varphi}^2\right] dF dx + \frac{1}{2}\int_0^l \rho(x)\dot{\theta}^2 \left(\int_F r^2 dF\right) dx \quad (8)$$

$$= \frac{1}{2} F \int_0^l \left[\rho(x)\left(\dot{u}^2 + \dot{\omega}^2\right)\right] dx + \frac{1}{2} I_y \int_0^l \rho(x)\dot{\varphi}^2 dx + \frac{1}{2} I_x \int_0^l \rho(x)\dot{\theta}^2 dx$$

where ρ(z) is mass density, θ is twist angle.

3. Construct FEM formular of the shaft

3.1 *Element stiffness matrix*

Considering the shaft element with two typical nodes (node i, node j) with length L, due to the deformation characteristics of the shaft, there will be four node displacements at each node. The global element vector of nodal displacements for a two-node genetic FGM element (i, j) has eight components as

$$\mathbf{d} = \left\{u_i \;\; \omega_i \;\; \varphi_i \;\; \theta_i \quad u_j \;\; \omega_j \;\; \varphi_j \;\; \theta_j\right\}^T \quad (9)$$

The displacements $u(x, t)$, $\omega(x, t)$, rotation $\varphi(x, t)$, and twist $\theta(x, t)$ are interpolated from the nodal displacements as

$$\begin{cases} u = \mathbf{N_u d} \\ \omega = \mathbf{N_\omega d} \\ \varphi = \mathbf{N_\varphi d} \\ \theta = \mathbf{N_\theta d} \end{cases} \rightarrow \begin{cases} u_{,x} = \mathbf{N_{u,x}.d} \\ \omega_{,x} = \mathbf{N_{\omega,x}.d} \\ \varphi_{,x} = \mathbf{N_{\varphi,x}.d} \\ \theta_{,x} = \mathbf{N_{\theta,x}.d} \end{cases} \quad (10)$$

where $\mathbf{N_u}$, $\mathbf{N_\omega}$, $\mathbf{N_\varphi}$ and $\mathbf{N_\theta}$ are the matrices of shape functions.

The element stiffness matrix is derived from the strain energy of an element U, and it has the form

$$U = \frac{1}{2}.F\int_0^l E(x) u_{,x}^2 dx + \frac{1}{2} I_y \int_0^l E(x)\omega_{,xx}^2 dx + \frac{1}{2} I_x \int_0^l G(x)\theta_{,x}^2 dx$$

$$= \frac{1}{2}\mathbf{d}^T\mathbf{d}\int_0^l \left[N_{u,x}^T E(x) N_{u,x} F + N_{\omega,xx}^T E(x) I_y N_{\omega,xx} + N_{\theta,x}^T G(x) I_x N_{\theta,x}\right] dx \quad (11)$$

$$= \frac{1}{2}\mathbf{d}^T\left(\mathbf{k_{aa}} + \mathbf{k_{bb}} + \mathbf{k_{ss}}\right)\mathbf{d} = \frac{1}{2}\mathbf{d}^T\mathbf{k}\mathbf{d}$$

$$\text{where} \quad \mathbf{k} = \mathbf{k}_{aa} + \mathbf{k}_{bb} + \mathbf{k}_{ss} \quad (12)$$

$$\mathbf{k}_{aa} = F\int_0^l \left[N_{u,x}^T E(x) N_{u,x} \right] dx \,,\ \mathbf{k}_{bb} = I_y \int_0^l \left[N_{\omega,xx}^T E(x) N_{\omega,xx} \right] dx \qquad (13)$$

$$\mathbf{k}_{ss} = I_x \int_0^l N_{\theta,x}^T G(x) N_{\theta,x} dx$$

3.2 *Element mass matrix*

The element mass matrix is derived from the shape functions for the displacement field. we write the kinetic energy (8) in the following form

$$\mathbf{T} = \frac{1}{2} F\int_0^l \rho(x)(\dot{u}^2 + \dot{\omega}^2) dx + \frac{1}{2} I_y \int_0^l \rho(x)\dot{\varphi}^2 dx + \frac{1}{2} I_x \int_0^l \rho(x)\dot{\theta}^2 dx$$

$$= \frac{1}{2}\dot{\mathbf{d}}^{\mathbf{T}}\dot{\mathbf{d}}\int_0^l \left[N_u^T \rho(x) N_u F + N_\omega^T \rho(x) N_\omega F + N_\varphi^T \rho(x) I_y N_\varphi + N_\theta^T \rho(x) I_x N_\theta \right] dx \qquad (14)$$

$$= \frac{\mathbf{1}}{\mathbf{2}}\dot{\mathbf{d}}^{\mathbf{T}}.\mathbf{m}.\dot{\mathbf{d}} = \frac{\mathbf{1}}{\mathbf{2}}\dot{\mathbf{d}}^{\mathbf{T}}\left(\mathbf{m}_{uu} + \mathbf{m}_{\omega\omega} + \mathbf{m}_{\varphi\varphi} + \mathbf{m}_{\theta\theta}\right)\dot{\mathbf{d}}$$

In which $\mathbf{m} = \mathbf{m}_{uu} + \mathbf{m}_{\omega\omega} + \mathbf{m}_{\varphi\varphi} + \mathbf{m}_{\theta\theta}$ is the mass matrix for an element.

Where

$$\mathbf{m}_{uu} = F\int_0^l N_u^T \rho(x) N_u dx \qquad \mathbf{m}_{\omega\omega} = F\int_0^l N_\omega^T \rho(x) N_\omega dx$$

$$\mathbf{m}_{\varphi\varphi} = I_y \int_0^l N_\varphi^T \rho(x) N_\varphi dx \,, \quad \mathbf{m}_{\theta\theta} = I_x \int_0^l N_\theta^T \rho(x) N_\theta dx \qquad (15)$$

$\mathbf{m}_{uu}$, $\mathbf{m}_{\omega\omega}$, $\mathbf{m}_{\varphi\varphi}$, $\mathbf{m}_{\theta\theta}$ are the axial mass matrix, the transverse mass matrix, the bending mass matrix, and the twisting mass matrix, respectively.

The equations of motion for 2D-FGM shaft can be written in the context of the finite element analysis as [11–13]

$$\mathbf{M}\ddot{\mathbf{D}} + \mathbf{K}\mathbf{D} = \mathbf{F} \qquad (16)$$

where $\mathbf{D}$, $\ddot{\mathbf{D}}$ are the total vectors of nodal displacements and accelerations. **M, K** and **F** are the mass matrix, the stiffness matrices and the nodal load vector of the shaft, respectively.

4. Numerical results and discussion

A computer code based on the developed formulation (16) and Newmark numerical algorithm [13,14] is developed and employed to study the dynamic behavior of the shaft in this Section Computations are carried out on FGM shaft made of steel SUS304 and aluminium Al_2O_3. Assume the mechanical properties of the material change from the left to end of the shaft, the left of the shaft is steel material, and the right end of the shaft is purely ceramic (Fig.1). To investigate the effect of shear strain and twist strain, for illustration, there is considered the shaft with constant cross-section, and shaft containing gear in the middle. The average radius of the gear is R, and the shaft has the following parameters: L = 0,5 (m), d = 0,02 (m), R = 0,06 m, the forces acting on the shaft at the midpoint of the shaft have the form $P = P_0.\cos(\Omega t)$; $M = R.P_0.\cos(\Omega t)$; P_0 = 2000 (N). The material data for constituents are as follows: $E_m = 2{,}1.10^{11}$ (N/m^2), $G_m = 8.10^{10}$ (N/m^2), ρ_m = 7860 (kg/m^3), $E_c = 3{,}8.10^{11}$ (N/m^2), $G_c = 18.10^{10}$ (N/m^2), ρ_c = 3960 (kg/m^3).

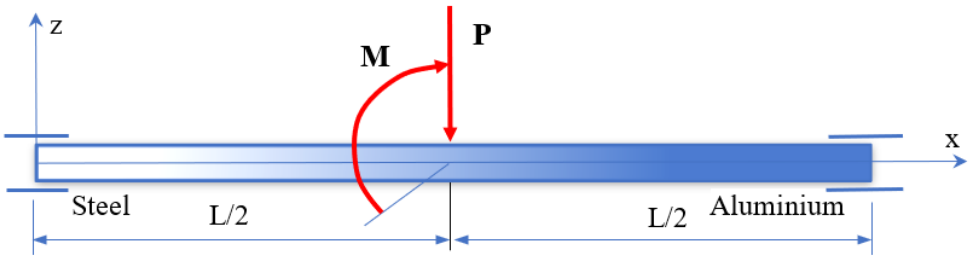

Figure 1. FGM shaft with dynamic loads

4.1 *Testing the calculation program and numerical algorithm*

To ensure the accuracy and convergence of the finite element model as well as the applied numerical algorithm, the FEM numerical results of the mathematical model built in the above section will be compared with the traditional analytical (GT) results. For simplicity, we consider the case of the problem where mechanical properties are constant: $E_c = E_m = E = 2.10^{11}$ (N/m^2); $G_c = G_m = 8.10^{10}$ (N/m^2); $\rho_m = \rho_c = 7860$ (kg/m^3)

The maximum deflection and torsion angle of the shaft with a homogeneous material calculated by the traditional analytical method is calculated by the formula [16]:

$$z_{max} = \frac{P_0 L^3 \cos(\Omega t)}{24{,}65.E.I_y} \tag{17}$$

$$\varphi_{max} = \frac{P_0 RL\cos(\Omega t)}{2.G.I_x} \tag{18}$$

Table 1. Comparison of the maximum deflection, torsion angle of the shaft by FEM and analytical results with Ω = 20 (rad/s)

Time (s)	FEM Deflection (m)	Analytical Deflection (m)	FEM Torsion (rad)	Analytical Torsion (rad)
0	0.0063	0.0063	0.0234	0.0234
0.1	0.0026	0.0026	0.0098	0.0098
0.2	0.0041	0.0041	0.0153	0.0153
0.3	0.0060	0.0061	0.0225	0.0225
0.4	$9.11.10^{-4}$	$9.22.10^{-4}$	0.0034	0.0034
0.5	0.0053	0.0053	0.0197	0.0197
0.6	0.0053	0.0053	0.0198	0.0198
0.7	$8.56.10^{-4}$	$8.66.10^{-4}$	0.0032	0.0032
0.8	0.0060	0.0061	0.0224	0.0224
0.9	0.0041	0.0042	0.0155	0.0155
1	0.0026	0.0026	0.0096	0.0096

Table 2. Comparison of the maximum deflection, torsion angle of the shaft by FEM and analytical results with Ω = 60 (rad/s)

Time (s)	FEM Deflection (m)	Analytical Deflection (m)	FEM Torsion (rad)	Analytical Torsion (rad)
0	0.0063	0.0063	0.0234	0.0234
0.1	0.0060	0.0061	0.0225	0.0225
0.2	0.0053	0.0053	0.0198	0.0198
0.3	0.0041	0.0042	0.0155	0.0155
0.4	0.0027	0.0027	0.0099	0.0099
0.5	$9.66.10^{-4}$	$9.77.10^{-4}$	0.0036	0.0036
0.6	$8.01.10^{-4}$	$8.11.10^{-4}$	0.0030	0.0030

0.7	0.0025	0.0025	0.0094	0.0094
0.8	0.0040	0.0041	0.0150	0.0150
0.9	0.0052	0.0053	0.0194	0.0194
1	0.0060	0.0060	0.0223	0.0223

The results in Tables (1–2) with different frequencies when comparison of deflection and torsion angle calculated by the FEM method and traditional analytical method shows the reliability and accuracy of the FEM. However, in the case of mechanical properties of variable materials (or FGM materials), analytical results are not available, so using the FEM is the best method to simulate the kinematic behavior of the shaft structure.

4.2 *Relationship between maximum shaft deflection and time*

The relationships between the shaft deflection over time with the different frequencies of the excitation forces are shown in the Figure 2. From these results, it can be seen that the dependence of the maximum deflection on the frequency of the excitation force is quite clear. The number of vibrations which the shaft executes increase with increasing the excitation frequency. When paying attention to the vibration amplitude over time of the largest deflection, we also see the dependence of the vibration amplitude on the material parameter (n), specifically when n is small (n = 1), the deflection has a larger amplitude than the amplitude with high material parameter (n = 5). That means, the vibration amplitude decreases when increasing the material parameter (n). However, the number of cycles performing the oscillation does not depend on the material parameter but on the frequency of the excitation force, the material parameter affects the amplitude of the oscillation.

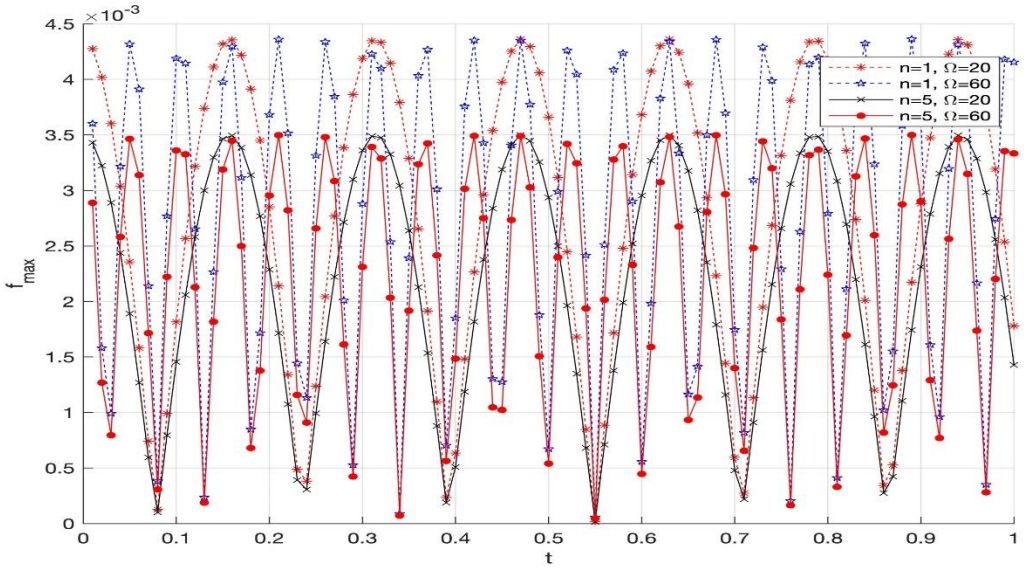

Figure 2. Relationship between maximum deflection (m) and time t(s)

4.3 *Relationship between the maximum torsion angle of the shaft and time*

The effect of the material parameter (n) and the oscillation frequency (Ω) on the torsional vibration of the FGM shaft can be seen in Fig. 3. Similar to the horizontal oscillation described above, the number of the torsional vibrations which the shaft executes increase with increasing the excitation frequency and the vibration amplitude decreases when increasing the material parameter (n).

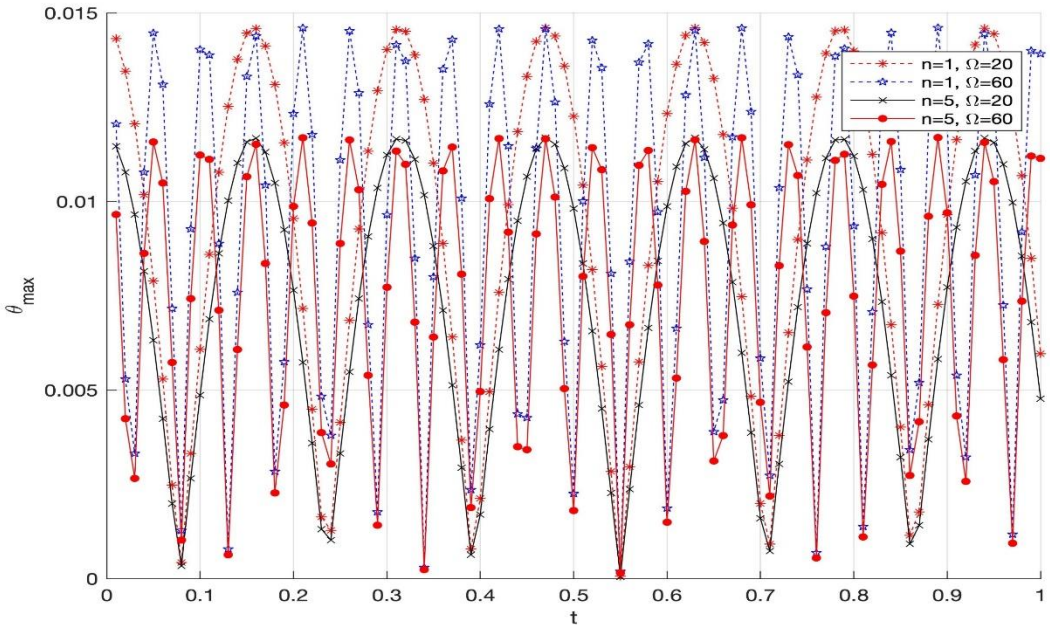

Figure 3. Relationship between maximum torsion angle (rad) and time t(s)

4.4 *Natural frequency of oscillation*

We consider the fundamental frequency parameter of the dimensionless horizontal oscillation of the shaft, which defined by [2]:

$$\mu = \omega_1 L^2 \sqrt{\frac{\rho_m A}{E_m J_y}} \tag{19}$$

where ω_1 is the fundamental horizontal oscillation frequency of the shaft.

The fundamental frequency parameter of the dimensionless torsional oscillation of the shaft has the form:

$$\gamma = \psi_1 L \sqrt{\frac{\rho_m}{G_m}} \tag{20}$$

where ψ_1 is the fundamental torsional frequency of the shaft.

The convergence of the fundamental frequency parameters received in Tables (3÷4) can be seen in that the numerical program converges quite quickly with a grid of 30 elements with all variable values of the material parameters. It is also possible to see the effect of the material parameter on the fundamental vibrational frequencies of the shaft. As the material parameter n increases, the fundamental frequencies also increase, which is consistent with the fact that the stiffness of the shaft increases as the frequency n increases.

Table 3. Convergence of the fundamental transverse oscillation frequency parameter μ

n	Number of Elements (nELE)					
	6	10	16	20	30	40
0.2	10.7725	10.7719	10.7719	10.7719	10.7719	10.7719
0.5	11.8941	11.8935	11.8934	11.8934	11.8934	11.8934
1	13.3539	13.3531	13.3530	13.3530	13.3530	13.3530
2	15.3056	15.3045	15.3044	15.3044	15.3044	15.3044
3	16.4702	16.4690	16.4688	16.4688	16.4688	16.4688
4	17.1838	17.1826	17.1824	17.1824	17.1824	17.1824
5	17.6343	17.6330	17.6328	17.6328	17.6328	17.6328

Tab 4. Convergence of fundamental torsion oscillation frequency parameter γ

n	Number of Elements (nELE)					
	6	10	16	20	30	40
0.2	1.6028	1.5973	1.5966	1.5965	1.5964	1.5964
0.5	1.7735	1.7671	1.7663	1.7662	1.7661	1.7661
1	1.9721	1.9646	1.9636	1.9635	1.9634	1.9634
2	2.2011	2.1920	2.1909	2.1908	2.1907	2.1907
3	2.3283	2.3185	2.3173	2.3171	2.3171	2.3171
4	2.4108	2.4005	2.3992	2.3991	2.3990	2.3990
5	2.4689	2.4585	2.4572	2.4570	2.4570	2.4570

5. Conclusions

The article has built a FEM model for the circular shaft element under the effect of harmonic force with mechanical properties changing along the longitudinal shaft. The finite element model is built based on Bernoulli's theory, which is quite commonly used in engineering and gives high reliability.

Building elastic deformation energy functions, and kinetic energy functions for variable mechanical shafts. From there, it is possible to build FEM formulas such as stiffness matrix, and mass matrix. Based on the FEM method combined with the Newmark digital algorithm has built a numerical program by Matlab software, which helps to simulate the kinematic behavior of the shaft.

The results obtained from the FEM equation using numerical algorithms and Matlab software give reliable results when compared with the results of the analytical method and the results of the convergence of the frequency parameter. Through the simulation results, it is possible to select the material parameter along with the excitation force frequency suitable for each problem with the structure or axial detail, thereby increasing or decreasing the vibration according to the wishes of the user.

Conflict of interest

There is no conflict of interest for this study.

References

[1] Şimşek, M. Vibration analysis of a functionally graded beam under a moving mass by using different beam theories. *Compos. Struct.* **2010**, *92*, 904–917, https://doi.org/10.1016/j.compstruct.2009.09.030.

[2] Şimşek, M.; Kocatürk, T. Free and forced vibration of a functionally graded beam subjected to a concentrated moving harmonic load. *Compos. Struct.* **2009**, *90*, 465–473, https://doi.org/10.1016/j.compstruct.2009.04.024.

[3] Rajabi, K.; Kargarnovin, M.H.; Gharini, M. Dynamic analysis of a functionally graded simply supported Euler–Bernoulli beam subjected to a moving oscillator. *Acta Mech.* **2012**, *224*, 425–446, https://doi.org/10.1007/s00707-012-0769-y.

[4] Nguyen Dinh Kien, Tran Thanh Hai. Dynamic analysis of prestressed Bernoulli beams resting on two-parameter foundation under moving harmonic load, Vietnam Journal of Mechanics, 28, pp. 176-188, (2006).

[5] Chang M Y, Chen J K, Chang C Y A. simple spinning laminated composite shaft model. International Journal of Solids and Structures, Vol. 41, p. 637-662, (2004).

[6] Chen, L.-W.; Peng, W.-K. DYNAMIC STABILITY OF ROTATING COMPOSITE SHAFTS UNDER PERIODIC AXIAL COMPRESSIVE LOADS. *J. Sound Vib.* **1998**, *212*, 215–230, https://doi.org/10.1006/jsvi.1997.1405.

[7] Y S Lee, Y W Kim. Nonlinear free vibration analysis of rotating hybrid cylindrical shells, Computers and Structures, Vol. 70, 161–168, (1999).

[8] Boukhalfa, A.; Hadjoui, A. Free vibration analysis of an embarked rotating composite shaft using the hp-version of the FEM. *Lat. Am. J. Solids Struct.* **2010**, *7*, 105–141, https://doi.org/10.1590/S1679-78252010000200002.

[9] Boukhalfa, A. Dynamic analysis of a spinning functionally graded material shaft by the p - version of the finite element method. *Lat. Am. J. Solids Struct.* **2014**, *11*, 2018–2038, https://doi.org/10.1590/s1679-78252014001100007.
[10] Nguyen Dinh Kien, Tran Thi Thom, A corotational formulation for large displacement analysis of functionally graded sandwich beam and frame structures, Mathematical Problems in Engineering, (2016).
[11] T J R Hughes. The finite element method. Linear static and dynamic finite element analysis. Dover publication Inc, Mineola, (2000).
[12] Shames, I.H.; Dym, C.L.; Saunders, H. Energy and Finite Element Methods in Structural Mechanics. *J. Vib. Acoust.* **1988**, *110*, 416–417, https://doi.org/10.1115/1.3269537.
[13] Daryl L, Logan A first course in the Element Finite Method, 4th Edition, Thomson Canada Limited, (2007).
[14] Kwon, Y.W.; Bang, H. The Finite Element Method Using MATLAB. **2018**, https://doi.org/10.1201/9781315275949.
[15] D C Pham. Essential solid mechanics. Institute of Mechanics, Hanoi, (2013).
[16] Nguyen Van Khang. Mechanical Vibration. Science and technics publising house, Viet Nam, (2004).